Influence of alloy composition and interlayer thickness on twist and tilt mosaic in $Al_xGa_{1-x}N$/AlN/GaN heterostructures

T. A. Lafford
Bede Scientific Instruments Ltd., Belmont Business Park, Durham DH1 1TW, United Kingdom

P. J. Parbrook
Department of Electrical and Electronic Engineering, University of Sheffield, Mappin Street, Sheffield S1 3JD, United Kingdom

B. K. Tanner[a]
Department of Physics, University of Durham, South Road, Durham DH1 3LE, United Kingdom

(Received 21 July 2003; accepted 10 November 2003)

High-resolution x-ray diffraction, in surface symmetric, skew symmetric, and grazing incidence in-plane diffraction geometries, has been used to investigate the effect of an AlN interlayer between micron thick GaN and $Al_xGa_{1-x}N$ layers grown by metalorganic vapor phase epitaxy on basal plane sapphire. No change is found in the tilt mosaic (threading screw dislocation density) with thickness or Al fraction x of the upper layer. A linear increase in the twist mosaic (threading edge dislocation density) was observed as a function of interlayer thickness and x. For all samples the twist mosaic of the AlGaN was significantly greater, by at least a factor of two, than that of the GaN layer. With increasing interlayer thickness the in-plane lattice parameter of the AlGaN decreased. The results are explained in terms of extra threading edge dislocations resulting from relaxation at the GaN/AlN interface. © *2003 American Institute of Physics.* [DOI: 10.1063/1.1637717]

Commercially successful nitride devices have been fabricated on GaN buffer layers grown on sapphire, and other heteroepitaxial substrates, despite the relatively high dislocation density in the material. The performance range of these devices can be extended through use of AlGaN buffer layers, allowing control of the in-plane lattice parameter while retaining an ideally low threading dislocation density. One successful method of fabricating AlGaN buffer layers that act as templates for subsequent device structure growth, without the formation of cracks due the tensile strain between AlGaN and GaN,[1] is through the use of AlN interlayers. These relieve the stress between the GaN underlayer and the AlGaN layer on top,[2] although some increase in the edge dislocation density threading through the AlGaN layer was observed. The best device layer growth occurs with the thinnest AlN interlayer for which cracking does not occur. Such interlayers have been used successfully in Bragg reflector mirrors[3,4] and solar blind detectors.[5]

The mechanism of stress relief in interlayers is now receiving significant attention. Bläsing *et al.*[6] showed that for low temperature interlayers a thin 100 nm $Al_{0.21}Ga_{0.79}N$ was compressively stressed due to the effect of the interlayer, but that this was reversed at higher interlayer growth temperatures. They concluded that the lowering of the growth temperature leads to a decoherence of the growth between the GaN underlayer and AlGaN overlayer.

Growth of the epilayers used in the present study was carried out using low pressure metalorganic vapor phase epitaxy in a showerhead reactor. GaN was grown on basal plane sapphire substrates using a GaN low temperature nucleation layer followed by growth of ~1 μm GaN at 1035 °C. The temperature was lowered to 600 °C and the AlN interlayer deposited. The AlGaN growth (typically 1 μm) was carried out at a temperature of 1050 °C. The details of the sample structures are given in Table I. Two series of samples were grown. The first had the device buffer of composition $Al_{0.25}Ga_{0.75}N$ and AlN interlayer thicknesses of $80\ \text{Å} \leq d \leq 220\ \text{Å}$. The second had varying device buffer composition $Al_xGa_{1-x}N$, with $0.16 \leq x \leq 0.46$ and constant AlN interlayer thickness $d = 150\ \text{Å}$.

High resolution x-ray diffraction (HRXRD) measurements were performed on a dual source Bede D1 diffractometer using a Cu target Microsource® microfocus generator equipped with a polycapillary focusing optic of divergence 0.17°. Surface-symmetric HRXRD measurements were made with a symmetrically cut Ge 004 beam-conditioning crystal, giving a beam of 2 mm×2 mm on the sample. An asymmetrically cut Si 220 analyzer crystal of 12 arcsec acceptance permitted the separation of mosaic tilt from strain. Skew-symmetric reflections were used to determine the relaxation (by measurement of a and c lattice parameters) of the individual GaN and AlGaN buffer layers. Here, an asymmetrically cut Ge 004 beam-conditioner gave an ~0.3 mm×~2 mm spot on the sample; the same analyzer crystal was again used. The asymmetric Ge beam conditioner

TABLE I. Growth conditions and nominal structure.

Layer	Composition	Thickness	Growth temperature (°C)
Device buffer	$Al_xGa_{1-x}N$	~1 μm	1050
Interlayer	AlN	d	600
Growth buffer	GaN	~1 μm	1035
Nucleation	GaN	300 Å	
Substrate	Sapphire (00.1)	-	-

[a]Electronic mail: b.k.tanner@durham.ac.uk

 © 2003 American Institute of Physics
Downloaded 21 Apr 2011 to 129.234.252.66. Redistribution subject to AIP license or copyright; see http://apl.aip.org/about/rights_and_permissions

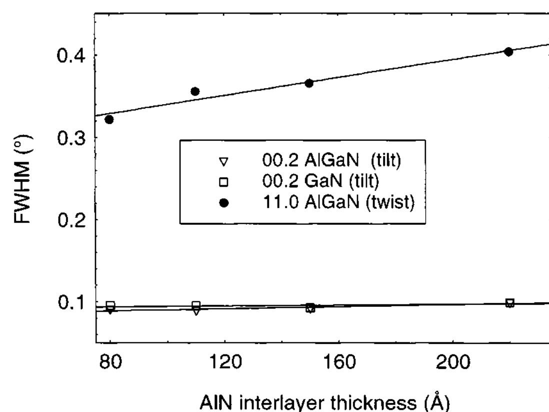

FIG. 1. Rocking curve FWHM vs interlayer thickness. Lines are linear least squares (LLSq) fits.

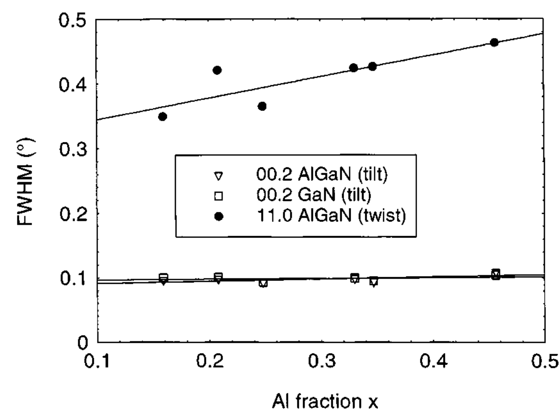

FIG. 2. Rocking curve FWHM vs Al fraction in the AlGaN layer. Interlayer thickness 150 Å. Lines are LLSq fits.

was also used for grazing incidence in-plane diffraction (GIIXD) measurements to determine the AlGaN tilt mosaic[7,8] and the in-plane lattice parameter; 0.4° acceptance Soller slits were used as an analyzer. Both for GIIXD and HRXRD geometries the instrumental resolution, determined using a single crystal silicon wafer, was over an order of magnitude smaller than the measured rocking curve widths.

Figure 1 shows the full width at half height maximum (FWHM) of the rocking curve versus interlayer thickness for the first set of samples. In the surface symmetric reflections we resolved the individual Bragg peaks associated with the GaN and AlGaN. For both layers, the rocking curves of the 00.2, 00.4, and 00.6 reflections were of almost identical shape and had FWHM within 6% of each other, there being no systematic trend with Bragg angle. This indicates that the FWHM is dominated by the mosaic spread. For surface symmetric reflections, the mosaic is pure tilt, associated with threading screw dislocations. Similarly, in the GIIXD measurements, the shape and FWHM of the 10.0, 20.0 and 11.0 rocking curves were almost equal, showing that the FWHM here determines the twist mosaic, associated with threading edge dislocations.[9] In GIIXD, where the incident beam incidence angle is below the critical angle for total external reflection, the evanescent wave does not penetrate more than a few nanometers and the 11.0 reflection rocking curve FWHM corresponds to the value of the twist mosaic spread of the AlGaN buffer. We note in Fig. 1 that the tilt mosaic, and hence the threading screw dislocation density, is equal for GaN and AlGaN buffer layers and independent of interlayer thickness. The twist mosaic of the AlGaN layer increases linearly with interlayer thickness and is significantly larger than the tilt mosaic.

The rocking curve FWHM versus the $Al_xGa_{1-x}N$ buffer layer composition in the second series of samples is displayed in Fig. 2. Again, the tilt mosaic is equal for the GaN and AlGaN layers and is independent of Al fraction in the AlGaN layer. There is also no change in the FWHM when the AlGaN is grown at 1080 °C, rather than 1050 °C. The FWHM of the 11.0 reflection, and hence twist mosaic, rises with Al fraction and is 3 or 4 times the value of the tilt mosaic.

The origin of the twist mosaic in the AlGaN must relate to the role of the interlayer. A series of skew symmetric reflections was taken for the sample with $x=0.46$ and $d=150$ Å to determine the twist mosaic in the buried GaN buffer layer. For this sample, the AlGaN layer is ~0.4 μm thick. The high resolution triple axis setting permits the scatter around the reciprocal lattice points associated with the GaN and AlGaN layers to be separated and the high incidence angle permits the GaN peak to be independently observed in the rocking curve. However, skew symmetric reflection rocking curves contain contributions from both tilt and twist mosaic and it is necessary to extrapolate the FWHM values to a skew angle of 90° in order to determine the twist mosaic. This has been done in Fig. 3, using the model of Srikant *et al.*[10] For the GaN layer, the twist mosaic is determined to be 0.16°, comparable with the tilt mosaic and much less than the twist mosaic of 0.46° in the corresponding AlGaN layer. The interlayer appears to add threading edge dislocations as has been observed using transmission electron microscopy by Amano and Akasaki.[2]

The twist mosaic in the GaN buffer layer arises from the threading components of the dislocations associated with the lattice mismatch between the nucleation layer and the sapphire substrate. There is initial island growth, with subsequent growth being equivalent to lateral overgrowth. The twist mosaic arises from the coalescence of the islands, giving blocks of high perfection separated by high dislocation density cell walls and rotated with respect to each other.

While the interlayer does not affect the tilt mosaic (threading screw dislocation density), there is a linear in-

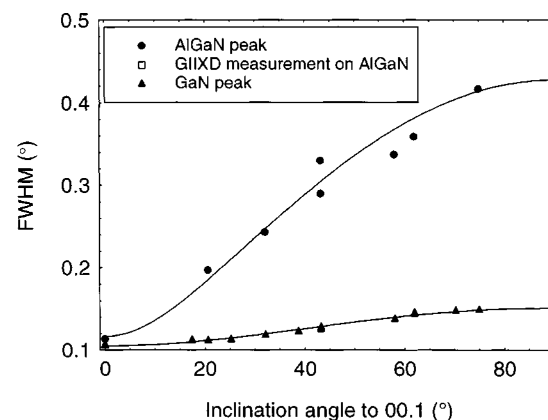

FIG. 3. FWHM of skew symmetric reflections from a sample with $x=0.46$ and $d=150$ Å. Solid lines are fits to Srikant's model with $m=0$ and Gaussian profiles.

Downloaded 21 Apr 2011 to 129.234.252.66. Redistribution subject to AIP license or copyright; see http://apl.aip.org/about/rights_and_permissions

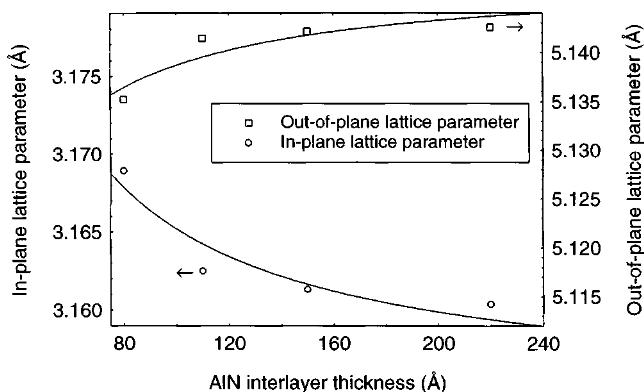

FIG. 4. a and c lattice parameters of the AlGaN layer vs interlayer thickness t. Solid lines are fits to the strain relief equation $y=A-(B/t)$, A and B being constants (Ref. 13).

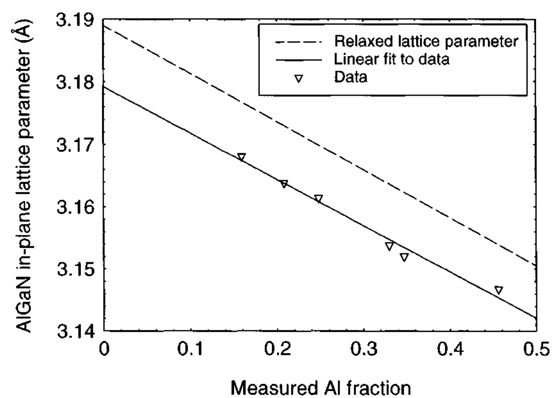

FIG. 5. In-plane a lattice parameter of the AlGaN layer vs aluminum fraction x (interlayer thickness 150 Å).

crease in twist mosaic with interlayer thickness. There is also a change in the in-plane lattice parameter of the AlGaN layer with interlayer thickness. From the analyzer peak position in the symmetric 00.2 and in-plane diffraction 11.0 reflections, the a and c lattice parameters as a function of the AlGaN layer thickness (Fig. 4) can be determined independently of the Al fraction.[11] As the interlayer thickness increases, the in-plane lattice parameter of the AlGaN layer decreases. It therefore becomes more strained with respect to the underlying AlN interlayer (assumed to be fully relaxed with respect to the GaN buffer). The variation in strain does not fit well the standard strain relief models, shown by the solid lines in Fig. 4, but the trend is similar. As observed by Bläsing *et al.*,[6] the AlGaN layer is seen to be compressively strained in-plane when the a lattice parameter is plotted against Al fraction x (Fig. 5). There is a linear fall in lattice parameter with x, and although the gradient is very close to that for relaxed $Al_xGa_{1-x}N$ there is a shift in absolute values.

The increase in twist mosaic in the AlGaN as a function of interlayer thickness cannot be associated with an increase in threading edge segments from additional misfit dislocations at the AlN/AlGaN interface. The additional threading edge dislocations appear to originate in the AlN layer. They could be associated with an increase in misfit dislocation density at the GaN/AlN interface as the AlN interlayer thickness increases. The best growth then occurs when the AlN interlayer has a minimum number of misfit and threading edge dislocations. However, this also corresponds to a maximum elastic strain, relieved beyond a critical threshold by cracking.

The increase in twist mosaic, and thus threading edge dislocation density, with increasing Al fraction in the AlGaN layer is less easy to explain. Increase of the Al content for a constant interlayer thickness decreases the lattice mismatch with respect to the AlN interlayer. The higher threading dislocation density for higher Al fraction therefore does not appear to be driven by relaxation between the AlN interlayer and the AlGaN layer. It has, however, been observed[12] that the surface morphology of the AlGaN layer changes as a function of the Al fraction. For higher Al content, the roughness correlation length decreases, implying that the size of the growth islands of the AlGaN on the AlN decreases. There is also an indication that the roughness amplitude increases with x. However, the increase in FWHM could only be explained by reduction of the diffracting domain size if the FWHM remained constant in reciprocal space. Our measurements show that the FWHM is constant in angular space.[9] If the reduction in domain size results in an increased FWHM, then it must also indicate an increase in the threading edge dislocation density associated with the smaller diffracting element boundaries.

Financial support for the GaN MOVPE growth program is acknowledged from EPSRC.

[1] R. T. Murray, P. J. Parbrook, and D. A. Wood, J. Mater. Sci. Lett. **22**, 113 (2003).
[2] H. Amano and I. Akasaki, Opt. Mater. (Amsterdam, Neth.) **19**, 219 (2002).
[3] F. Natali, D. Bryne, A. Dussaigne, N. Grandjean, J. Massies, and B. Daminterlayerano, Appl. Phys. Lett. **82**, 499 (2003).
[4] K. E. Waldrip, J. Han, J. J. Fiegel, H. Zhou, E. Makarona, and A. V. Nurmikko, Appl. Phys. Lett. **78**, 3205 (2001).
[5] C. Pernot, A. Hirano, M. Iwaya, T. Detchprohm, H. Amano, and I. Akasaki, Jpn. J. Appl. Phys., Part 2 **39**, L387 (2000).
[6] J. Bläsing, A. Reiher, A. Dadgar, A. Diez, and A. Krost, Appl. Phys. Lett. **81**, 2722 (2002).
[7] M. S. Goorsky and B. K. Tanner, Cryst. Res. Technol. **37**, 647 (2002).
[8] T. A. Lafford, P. A. Ryan, D. E. Joyce, M. S. Goorsky, and B. K. Tanner, Phys. Status Solidi A **195**, 265 (2003).
[9] T. A. Lafford, B. K. Tanner, and P. J. Parbrook, J. Phys. D **36**, A245 (2003).
[10] V. Srikant, J. S. Speck, and D. R. Clark, J. Appl. Phys. **82**, 4286 (1997).
[11] D. K. Bowen and B. K. Tanner, *High Resolution X-Ray Diffractometry and Topography* (Taylor and Francis, London, 1998), p. 252.
[12] P. J. Parbrook and T. Wang (unpublished).
[13] R. Beanland, D. J. Dunstan, and P. J. Goodhew, Adv. Phys. **45**, 87 (1996).

Downloaded 21 Apr 2011 to 129.234.252.66. Redistribution subject to AIP license or copyright; see http://apl.aip.org/about/rights_and_permissions